



## Resonance surface X-ray scattering technique to determine the structure of electrodeposited Pt ultrathin layers on Au(1 1 1) surface

Toshihiro Kondo<sup>a,\*</sup>, Masayo Shibata<sup>a</sup>, Naoko Hayashi<sup>a</sup>, Hitoshi Fukumitsu<sup>b</sup>, Takuya Masuda<sup>b</sup>, Satoru Takakusagi<sup>b</sup>, Kohei Uosaki<sup>b,c,\*</sup>

<sup>a</sup> Division of Chemistry, Graduate School of Humanities and Sciences, Ochanomizu University, Ohtsuka, Bunkyo-ku, Tokyo 112-8610, Japan

<sup>b</sup> Physical Chemistry Laboratory, Division of Chemistry, Graduate School of Science, Hokkaido University, Sapporo 060-0810, Japan

<sup>c</sup> International Center for Materials Nanoarchitectonics (MANA) Satellite, National Institute for Materials Science (NIMS), Sapporo 060-0810, Japan

### ARTICLE INFO

#### Article history:

Received 28 November 2009

Received in revised form 26 April 2010

Accepted 2 May 2010

Available online 11 May 2010

#### Keywords:

Au(1 1 1) single crystal electrode

Electrochemical deposition of Pt

Resonance surface X-ray scattering (RSXS)

Surface atomic arrangement

Pseudomorphic layer

### ABSTRACT

It is demonstrated that resonance surface X-ray scattering (RSXS), in which incident X-ray energy close to the Pt L<sub>III</sub> absorption edge (11.55 keV) is used, is very useful for the determination of the structure of electrodeposited Pt thin layers on a Au(1 1 1) surface. This technique was applied to characterize the structure of electrodeposited Pt layers on Au(1 1 1) substrates prepared under two extreme conditions, which are known to provide rough and atomically flat layers. Detailed structural information was obtained by RSXS measurements and it was confirmed that the structures of the Pt layers were as reported. Pt atoms of the atomically flat monolayer were found to be situated at the threefold hollow cubic closest packing (ccp) sites of the Au(1 1 1)-(1 × 1) surface.

© 2010 Elsevier Ltd. All rights reserved.

### 1. Introduction

Ultrathin metal layers on foreign metal substrates have been attracting interests because of their unique physical and chemical properties, particularly their high electro-catalytic activities [1,2]. Such high electro-catalytic activities are caused by the geometric and electronic structures of the interfacial layers different from those of the bulk [3], and therefore, it is very important to know the interfacial structures with atomic dimensions. The interfacial structures of electrochemically deposited ultrathin metal layers on foreign metal substrates have been investigated using various techniques, such as scanning probe microscopy (SPM) such as scanning tunneling microscopy (STM) and atomic force microscopy (AFM) [4–20] and several optical techniques [16,20–24]. Although SPM measurements provide structural information with an atomic resolution, only information of the outermost layer can be obtained, while the structure at the interface between the electrodeposited metal layer and substrate surface cannot be determined by SPM. Information obtained by optical techniques contains contributions not only from the electrode surface, but also from the bulk.

The surface X-ray scattering (SXS) technique is known to be one of the best methods to investigate the interfacial structure at an atomic level as the structural information of not only the overlayer, but also of the substrate can be obtained [25–30]. We have already carried out the structural investigation of underpotentially deposited (UPD) Pd ultrathin films on Au(1 1 1) and Au(1 0 0) using *in situ* STM and SXS techniques and discussed the relationship between the interfacial structure and the electrochemical properties [3,31–33]. We have also studied the structure [34] and stability [35] of a UPD Ag ultrathin layer on a Au(1 1 1) surface using the *in situ* SXS technique.

Pt ultrathin layers on foreign metal substrates are expected to be a good electrocatalyst in many areas. Although the structural studies of electrochemically deposited Pt ultrathin layers on a Au(1 1 1) single crystal electrode surface have been carried out by several groups [9–12] using STM, the results were different from each other. While Naohara et al. reported that Pt grows on an atomically flat Au(1 1 1) surface in the Frank–van der Merwe (FM; layer-by-layer) mode [12], Waibel et al. [9] and Strbac et al. [10] reported that Pt grows on the Au(1 1 1) surface in the Volmer–Weber (VW; islanding) mode. A more precise structural investigation is required to discuss the deposition mechanism.

The SXS technique is ideal to determine the structure of the metal deposits with atomic precision as mentioned above, but since the atomic number and, therefore, the scattering parameters of Pt

\* Corresponding author.

E-mail address: [uosaki.kohei@nims.go.jp](mailto:uosaki.kohei@nims.go.jp) (K. Uosaki).

are too close to those of Au, the interfacial structure of the Pt layer on the Au substrate cannot be precisely determined from the (00) rod data obtained using the incident X-ray energy of 11.271 keV, which is usually used in our SXS studies [30–37].

We have now demonstrated that the resonance SXS (RSXS) method, in which the incident X-ray energy close to the Pt  $L_{III}$  absorption edge (11.55 keV) is used so that the anomalous scattering parameter effect is utilized [38–41], is very useful to precisely determine the interfacial structure of the Pt layers deposited on the Au(1 1 1) surface by applying this technique to the electrodeposited Pt on a Au(1 1 1) surface prepared under two extreme conditions as already reported; one to form a rough Pt layer [9,10] and the other to form an atomically flat Pt layer [12].

## 2. Experimental

### 2.1. Materials

A Au(1 1 1) single crystal disk (diameter: 10 mm, thickness: 5 mm) was purchased from the Surface Preparation Laboratory (The Netherlands) and used after the previously described pre-treatments [30,35,42]. Pt wire and Pt foil were purchased from Nilaco. Ultrapure reagent grade  $H_2SO_4$  and  $HClO_4$ , reagent grade  $K_2PtCl_4$ , and reagent grade  $H_2PtCl_6$  were purchased from Wako Pure Chemicals, Aldrich, and Sigma, respectively, and were used without further purification. Water was purified using a Milli-Q system (Yamato, WQ-500). Ultrapure  $N_2$  (99.9995%) was purchased from Tomoe Shokai.

### 2.2. Electrochemical deposition of Pt on Au(1 1 1)

Before the Pt deposition, the Au(1 1 1) disk was annealed using a Bunsen burner, cooled in a quartz vessel for a few minutes and then quenched in ultrapure water. A Pt wire and Hg/Hg<sub>2</sub>SO<sub>4</sub> electrode (MSE, double junction) were used as the counter and reference electrodes, respectively. The electrode potential was controlled and the current was recorded by a CompactStat (Ivium).

The Pt was electrochemically deposited on the Au(1 1 1) disk under two extreme conditions so that smooth and rough deposits were obtained as reported by previous reports.

In the first method, the deposition was carried out in a 0.1 M  $HClO_4$  solution containing 0.5 mM  $K_2PtCl_4$  and the electrode potential was negatively scanned from the open circuit potential (OCP) to a certain pre-determined potential at the scan rate of  $5\text{ mV s}^{-1}$  [9,10]. The Au(1 1 1) disk was removed from the electrochemical cell as soon as the potential reached the pre-determined potential. The sample obtained with the negative potential limit of  $-0.15\text{ V}$  (vs. MSE) was used for the RSXS study as Pt/Au(1 1 1)<sub>1</sub>,<sup>1</sup> which is expected to be rough according to previous reports [9,10].

In the second method, the deposition was carried out in a 0.1 M  $HClO_4$  solution containing 0.05 mM  $H_2PtCl_6$ . The electrode potential was negatively scanned from OCP to  $-0.02\text{ V}$  at the scan rate of  $2\text{ mV s}^{-1}$ , kept at this potential for a certain pre-determined time [12] and then the Au(1 1 1) disk was removed from the electrochemical cell. The sample obtained with the deposition time of

2000 s was used for the RSXS study as Pt/Au(1 1 1)<sub>2</sub>,<sup>2</sup> which is expected to be atomically flat according to a previous report [12].

### 2.3. RSXS measurements

The RSXS measurements were carried out at the bending-magnet beamline BL4C at the Photon Factory. After the Pt deposition, the Au(1 1 1) disk was rinsed with conc.  $H_2SO_4$  and ultrapure water in order to remove the adsorbed  $PtCl_4^{2-}$  or  $PtCl_6^{4-}$ , dried by blowing  $N_2$  gas, and then placed in the SXS cell [35,36]. The SXS cell was mounted on a six-circle diffractometer (HUBER, 5020) installed at the beamline. X-ray radiation was monochromated by a Si(1 1 1) double-crystal system and its energy was calibrated using the absorption edge energy of a Pt foil. The X-ray beam was focused by a Rh-coated bending mirror. The beam size of the incident X-ray, which can be adjusted by a slit placed in front of the cell, was  $0.1\text{--}0.2\text{ mm}$  (vertical)  $\times$   $0.2\text{--}0.5\text{ mm}$  (horizontal). The beam size of the scattered X-ray was  $0.05\text{--}0.1\text{ mm}$  (vertical)  $\times$   $0.1\text{--}0.2\text{ mm}$  (horizontal) as adjusted by a slit, which was placed in front of a detector (NaI scintillation counter) to avoid any fluorescence from the Pt layers. The energy range of the incident X-ray was selected to be between 11.40 and 11.75 keV in order to contain the Pt  $L_{III}$  absorption edge (11.55 keV). It was confirmed that the beam position was not out of position during changing the incident X-ray energy between 11.40 and 11.75 keV. The intensity of the incident X-ray was measured by an ion chamber, which was placed in front of the sample, to normalize the data. All the RSXS measurements were carried out in such a mode that the incoming and outgoing angles with respect to the sample surface were equal. At each measuring point, a rocking scan of the  $\omega$ -axis was performed for the background subtraction and for the integration over the mosaic spread of the sample. Ultrapure  $N_2$  gas was flowed into the cell during the RSXS measurements to avoid X-ray induced formation of active species such as ozone and radicals [35].

A reciprocal coordinate system ( $H$ ,  $K$ ,  $L$ ) with two components ( $H$  and  $K$ ) lying parallel to the surface and the other one ( $L$ ) along the surface normal was used in this study. Structures along the direction normal to the surface were quantitatively determined from the least-square fitting to the (00) rod, (01) rod, and energy dependence data with a kinematic calculation based on a specific interfacial model [30,31,33–37] consisting of three layers on top of the Au(1 1 1)-(1  $\times$  1) substrate. When the Pt layers were made in contact with the electrolyte solution after the expose to the air at the Pt–O reduction potential, no cathodic current was observed. Thus, only Pt and Au were considered in the fitting. The in-plane structures of the Pt layer on the Au(1 1 1)-(1  $\times$  1) surface were also determined by comparing the experimentally obtained (0 1) rod data with those calculated for two different structures with the position of the Pt atoms of the first layer at (1) the cubic closest packing (ccp) sites, and (2) the hexagonal closest packing (hcp) sites of the Au(1 1 1) substrate. Coverage in each layer is described using ML as a unit where 1 ML corresponds to  $1.39 \times 10^{15}$  atoms  $\text{cm}^{-2}$ .

## 3. Results and discussion

Fig. 1 shows the (00) rods of (a) Pt/Au(1 1 1)<sub>1</sub> and (b) Pt/Au(1 1 1)<sub>2</sub> samples and Fig. 2 shows (a) (01) rods and (b) the

<sup>1</sup> The Au(1 1 1) disk removed from the deposition cell was transferred to another cell containing a 0.05 M  $H_2SO_4$  solution after being rinsed with pure water and conc.  $H_2SO_4$ . Cyclic voltammograms (CVs) were then recorded. The CVs showed that the cathodic charge due to the Au oxide reduction decreased as the negative potential limit became more negative, indicating that the free Au site decreased as Pt was deposited, but no further decrease was observed even if the negative potential limit was made more negative than  $-0.15\text{ V}$ . Thus, we chose the sample obtained with the negative potential limit of  $-0.15\text{ V}$  for the RSXS study as Pt/Au(1 1 1)<sub>1</sub>. During the preparation of the Pt/Au(1 1 1)<sub>1</sub>, ca. 1.7 ML of Pt was deposited on the Au(1 1 1) surface based on the cathodic charge.

<sup>2</sup> The Au(1 1 1) disk removed from the deposition cell was transferred to another cell containing a 0.05 M  $H_2SO_4$  solution after being rinsed with pure water and conc.  $H_2SO_4$ . The CVs were then recorded. The CVs showed that the cathodic charge due to the Au oxide reduction decreased as the deposition time increased, indicating a decrease in the free Au site as already described in footnote 1, but no further decrease was observed after a 2000 s deposition time. Thus, we chose the sample obtained with the deposition time of 2000 s for the RSXS study as Pt/Au(1 1 1)<sub>2</sub>.

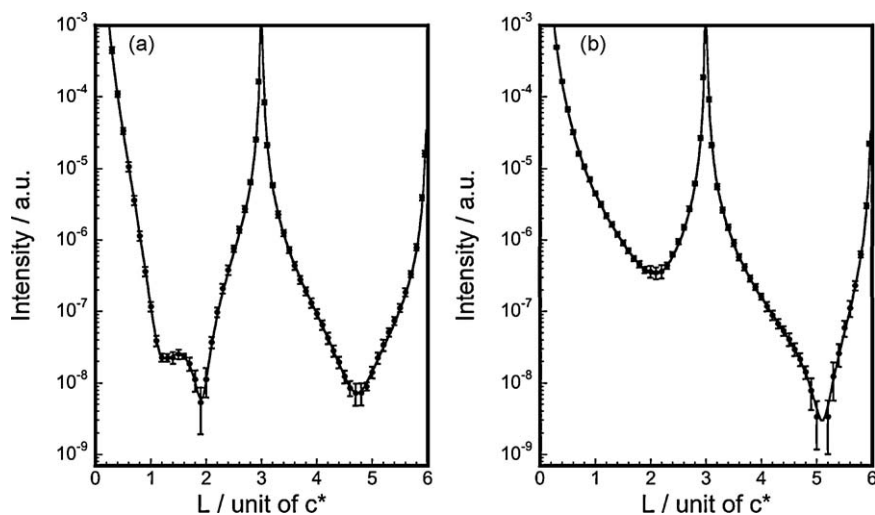


**Fig. 1.** (00) rod profiles of (a) Pt/Au(111)<sub>1</sub> and (b) Pt/Au(111)<sub>2</sub> samples. The circles and the solid lines are the experimental data and the calculated curves fitted by the least-squares method with a kinematic calculation, respectively. The standard error values of the scattered X-ray intensity are shown as error bars in the figure.

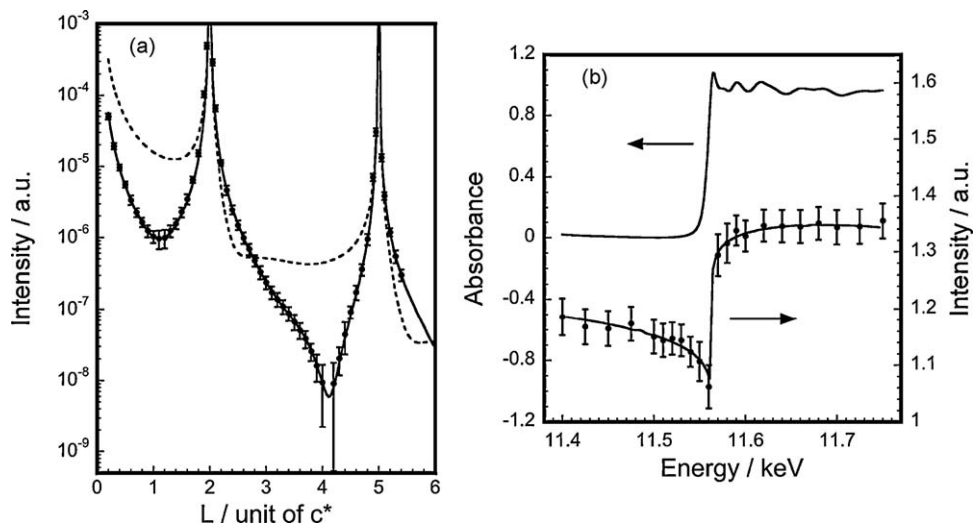


**Fig. 2.** (a) (01) rod profile of Pt/Au(111)<sub>2</sub> and (b) energy dependence of scattered X-ray intensity at (000.5) of Pt/Au(111)<sub>2</sub>. The circles represent the experimental data and the solid line is the calculated curve fitted by the least-squares method with a kinematic calculation for the Pt adsorption on the ccp sites. The dotted line is the calculated curve for the Pt adsorption on the hcp site. The standard errors of the scattered X-ray intensity are shown as error bars in the figure. A Pt absorption spectrum, which was used as an energy reference, is also shown.

energy dependence of the scattered X-ray intensity at (000.5) of Pt/Au(111)<sub>2</sub>. The structural parameters obtained from the least-square fitting with a kinematical calculation are listed in Tables 1 and 2.

At Pt/Au(111)<sub>1</sub>, the best fit data from the (00) rod profile (Fig. 1(a)) show that three Pt layers are present on the Au(111)-(1 × 1) surface (Fig. 3(a)). The layer distance between the first Pt and the outermost Au layers is 0.230 nm, which is slightly larger than that calculated for the Pt layer with Pt atoms situated at the threefold hollow site on the Au(111)-(1 × 1) surface, 0.227 nm, but less than those calculated for the Pt layers with Pt atoms situated at the on-top, 0.283 nm, and bridge sites, 0.243 nm, on the Au(111)-(1 × 1) surface, showing that most of the Pt atoms in the first layer are at the threefold hollow site of the underlying Au(111)-(1 × 1) surface. The layer distances between the first and second and the second and third Pt layers are 0.227 and 0.228 nm, respectively, which are larger than that calculated for the Pt layer with Pt atoms situated at the threefold hollow site on the epitaxially formed Pt layer on the Au(111)-(1 × 1) surface, 0.221 nm, but less than those calculated for the Pt layers with Pt atoms situated at the on-top,

**Table 1**

Structural parameters obtained from the analyses of the (00) rod profile at Pt/Au(111)<sub>1</sub> as a three-layer model on Au(111)-(1 × 1).

<sup>a</sup>	
Distance, $z_{\text{Au-Pt}(1)}$ /nm	$0.230 \pm 0.008$
Distance, $z_{\text{Pt}(1)-\text{Pt}(2)}$ /nm	$0.228 \pm 0.010$
Distance, $z_{\text{Pt}(2)-\text{Pt}(3)}$ /nm	$0.227 \pm 0.009$
Coverage, $\rho_{\text{Pt}(1)}$ /ML	$0.93 \pm 0.06$
Coverage, $\rho_{\text{Pt}(2)}$ /ML	$0.71 \pm 0.09$
Coverage, $\rho_{\text{Pt}(3)}$ /ML	$0.26 \pm 0.13$
RMS, $\sigma_{\text{Pt}(1)}$ /nm	$0.032 \pm 0.003$
RMS, $\sigma_{\text{Pt}(2)}$ /nm	$0.086 \pm 0.007$
RMS, $\sigma_{\text{Pt}(3)}$ /nm	$0.141 \pm 0.040$

<sup>a</sup> The subscripts of Au, Pt(1), Pt(2), and Pt(3) represent the outermost Au layer, the first Pt layer, second Pt layer, and third Pt layer, respectively. Distances of  $z_{\text{Au-Pt}(1)}$ ,  $z_{\text{Pt}(1)-\text{Pt}(2)}$ , and  $z_{\text{Pt}(2)-\text{Pt}(3)}$  represent atomic layer distances between the Au substrate and first Pt layer, the first and second Pt layers, and the second and third Pt layers, respectively.

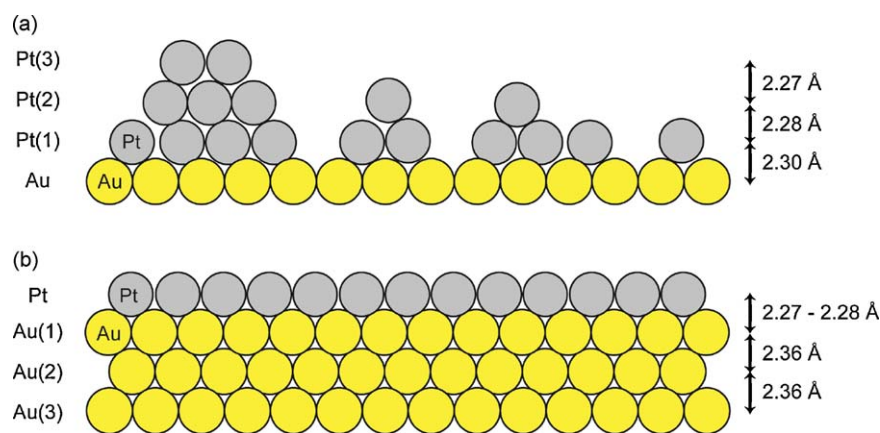


Fig. 3. Schematic side views of (a) Pt/Au(1 1 1).1 and (b) Pt/Au(1 1 1).2 based on the RSXS results.

0.277 nm, and bridge sites, 0.236 nm, on the epitaxially formed Pt layer on the Au(1 1 1)-(1 × 1) surface. These results indicated that the Pt atoms in the second and third Pt layers randomly situated on the first and second Pt layers, respectively. Coverage of the first, second, and third Pt layers are 0.93, 0.71, and 0.26 ML, respectively, indicating that the surface of Pt/Au(1 1 1).1 is very rough. The high RMS values also support the fact that the surface of the Pt deposited layers was very rough. This is in agreement with previous results [9,10]. Although there is a possibility of the formation of the small Pt clusters, in which Pt–Pt distances maybe smaller, we avoided the discussion about this in the present study because more detailed experimental data such as STM, X-ray absorption spectroscopy (XAS), grazing incidence X-ray scattering (GIXS) are required.

At Pt/Au(1 1 1).2, a dip was observed between the Bragg points in the (0 0) (Fig. 1(b)) and (0 1) (Fig. 2(a)) rods, suggesting that the Pt monolayer was formed on the Au(1 1 1) surface. The scattered X-ray intensity at (0 0 0.5) (Fig. 2(b)) was dependent on the incident X-ray energy, indicating that the outermost surface atom should be platinum. All the best fit data from the present results, i.e., the (0 0) and (0 1) rod profiles and energy dependence, showed the formation of an atomically flat Pt monolayer (0.96–0.98 ML) on the Au(1 1 1)-(1 × 1) surface (Fig. 3(b)), confirming the previous results [12]. The layer distance between the first Pt and the outermost Au layers is 0.227–0.228 nm, which is in good agreement with that calculated for the Pt layer with Pt atoms situated at the threefold hollow site on the Au(1 1 1)-(1 × 1) surface, 0.227 nm. There are two threefold

hollow sites on the Au(1 1 1)-(1 × 1) surface, i.e., the hcp site and the ccp site. While the (0 0) rod profile contains the information only of the structure normal to the surface, the (0 1) rod profile can be used to obtain information about the in-plane structure. In Fig. 2(a), the solid and dotted lines show the calculated curves fitted by the least-squares method with a kinematic calculation for the Pt adsorption on the ccp and hcp sites, respectively. It is clear that the fitting for the Pt atoms on the ccp site gives the best fit to the experimental data, indicating that the deposited Pt monolayer maintains the fcc stacking sequence of the Au(1 1 1) substrate. This behavior is the same as those in the case of the electrochemical deposition of Pd [30–32] and Ag [33,34] on the Au(1 1 1) surface.

#### 4. Conclusions

We demonstrated that resonance surface X-ray scattering (RSXS) is very useful to precisely determine the interfacial structure of Pt layers deposited on a Au(1 1 1) surface. The structures of electrodeposited Pt layers prepared on a Au(1 1 1) surface under two conditions were investigated. It was confirmed that a rough Pt multilayer and an atomically flat Pt monolayer, whose structures had already been reported by STM, were formed on the Au(1 1 1)-(1 × 1) surface. The Pt atoms of the atomically flat monolayer were found to be situated at the threefold hollow cubic closest packing (ccp) sites of the Au(1 1 1)-(1 × 1) surface. The *in situ* RSXS investigation during the Pt deposition is now under way.

#### Acknowledgements

We wish to thank Dr. Tamura of the Japan Atomic Energy Agency for his help with the CTR and energy dependence calculation and the fitting program. This work was partially supported by Grants-in-Aid for Scientific Research (A) (No. 18205016) to KU and (C) (No. 20550009) to TK from Japan Society of Promotion of Science (JSPS) and World Premier International Research Center (WPI) Initiative on Materials Nanoarchitectonics (MANA) from Ministry of Education, Culture, Sports, Science, and Technology (MEXT), Japan. The synchrotron radiation experiments were performed as projects approved by the Photon Factory Program Advisory Committee (PAC Nos. 2007G085, 2008G124, and 2009G038).

#### References

- [1] G.A. Somorjai, Surface Chemistry and Catalysis, John Wiley & Sons, New York, 1993.
- [2] A.W. Adamson, Physical Chemistry of Surface, 4th ed., John Wiley & Sons, New York, 1994.
- [3] H. Naohara, S. Ye, K. Uosaki, J. Electroanal. Chem. 500 (2001) 435.
- [4] N. Batina, T. Will, D.M. Kolb, Faraday Discuss. 94 (1992) 93.

Table 2

Structural parameters obtained from the analyses of the (0 0) and (0 1) rod profiles and energy dependence of (0 0 0.5) scattered intensity at Pt/Au(1 1 1).2 as a three-layer model on Au(1 1 1)-(1 × 1).

<sup>a</sup>	From (0 0) rod	From (0 1) rod	From energy dependence
Distance, $Z_{\text{Au}(3)-\text{Au}(2)}/\text{nm}$	0.236 <sup>b</sup>	0.236 <sup>b</sup>	0.236 <sup>b</sup>
Distance, $Z_{\text{Au}(2)-\text{Au}(1)}/\text{nm}$	0.236 ± 0.001	0.236 ± 0.01	0.236 ± 0.001
Distance, $Z_{\text{Au}(1)-\text{Pt}}/\text{nm}$	0.227 ± 0.002	0.228 ± 0.03	0.228 ± 0.005
Coverage, $\rho_{\text{Au}(2)}/\text{ML}$	1.00 <sup>b</sup>	1.00 <sup>b</sup>	1.00 <sup>b</sup>
Coverage, $\rho_{\text{Au}(1)}/\text{ML}$	0.99 ± 0.06	1.00 ± 0.01	0.99 ± 0.06
Coverage, $\rho_{\text{Pt}}/\text{ML}$	0.96 ± 0.08	0.98 ± 0.08	0.98 ± 0.08
RMS, $\sigma_{\text{Au}(2)}/\text{nm}$	0.008 ± 0.003	0.007 ± 0.003	0.009 ± 0.002
RMS, $\sigma_{\text{Au}(1)}/\text{nm}$	0.009 ± 0.006	0.010 ± 0.008	0.009 ± 0.002
RMS, $\sigma_{\text{Pt}}/\text{nm}$	0.017 ± 0.004	0.017 ± 0.005	0.017 ± 0.003

<sup>a</sup> The subscripts of Pt, Au(1), Au(2), and Au(3) represent the Pt layer, first outermost Au layer, second outermost Au layer, and third outermost Au layer, respectively. Distances of  $Z_{\text{Au}(3)-\text{Au}(2)}$ ,  $Z_{\text{Au}(2)-\text{Au}(1)}$ , and  $Z_{\text{Au}(1)-\text{Pt}}$  represent atomic layer distances between the third and second outermost Au layers, the second and first outermost Au layers, and the Au top and Pt layers, respectively.

<sup>b</sup> Fixed value in the fitting.

- [5] N. Shinotsuka, K. Sashikata, K. Itaya, *Surf. Sci.* 335 (1995) 75.
- [6] Y. Shingaya, H. Matsumoto, H. Ogasawara, M. Ito, *Surf. Sci.* 335 (1995) 23.
- [7] C.A. Jeffrey, D.A. Harrington, S. Morin, *Surf. Sci.* 512 (2002) L367.
- [8] S.R. Brankovic, J.X. Wang, R.R. Adžić, *Surf. Sci.* 474 (2001) L173.
- [9] H.-F. Waibel, M. Kleinert, L.A. Kibler, D.M. Kolb, *Electrochim. Acta* 47 (2002) 1461.
- [10] S. Strbac, S. Petrovic, R. Vasilic, J. Kobac, A. Zalar, Z. Rakocevic, *Electrochim. Acta* 53 (2007) 998.
- [11] A. Mathur, J. Erlebacher, *Surf. Sci.* 602 (2008) 2863.
- [12] K. Uosaki, S. Ye, H. Naohara, Y. Oda, T. Haba, T. Kondo, *J. Phys. Chem. B* 101 (1997) 7566.
- [13] H. Naohara, S. Ye, K. Uosaki, *J. Phys. Chem. B* 102 (1998) 4366.
- [14] H. Naohara, S. Ye, K. Uosaki, *J. Electroanal. Chem.* 473 (1999) 2.
- [15] S. Takakusagi, K. Kitamura, K. Uosaki, *J. Phys. Chem. C* 112 (2008) 3073.
- [16] R. Widmer, H. Siegenthaler, *Electrochem. Commun.* 7 (2005) 421.
- [17] E. Herrero, H.D. Abruña, *Langmuir* 13 (1997) 4446.
- [18] C.-H. Chen, S.M. Vesecky, A.A. Gewirth, *J. Am. Chem. Soc.* 114 (1992) 451.
- [19] S. Takami, G.K. Jennings, P.E. Laibinis, *Langmuir* 17 (2001) 441.
- [20] J.M. Delgado, J.M. Orts, A. Rodes, *Langmuir* 21 (2005) 8809.
- [21] H. Furukawa, K. Ajito, M. Takahashi, M. Ito, *J. Electroanal. Chem.* 280 (1990) 415.
- [22] T.J. Schmidt, B.N. Grgur, R.J. Behm, N.M. Markovic, P.N. Ross Jr., *Phys. Chem. Chem. Phys.* 2 (2000) 4379.
- [23] M. Futamata, *Chem. Phys. Lett.* 333 (2001) 337.
- [24] D.M. Kolb, in: R.J. Gale (Ed.), *Spectroelectrochemistry, Theory and Practice*, Plenum Press, New York, 1988.
- [25] M.F. Toney, O.R. Melroy, in: H.D. Abruña (Ed.), *Electrochemical Interfaces: Modern Techniques for in Situ Interfacial Characterization*, VCH Publishers, Inc., New York, 1991 (Chapter 2).
- [26] M.F. Toney, J. McBreen, *Interface, Electrochem. Soc.* 2 (Spring) (1993) 22.
- [27] M.F. Toney, in: C.A. Melendres, A. Tadjeddine (Eds.), *Synchrotron Techniques in Interfacial Electrochemistry*, NATO ASI Series, Kluwer Academic, Boston, 1994.
- [28] J. Wang, B.M. Ocko, A.J. Davenport, H.S. Isaacs, *Phys. Rev. B* 46 (1992) 10321.
- [29] J. Wang, A.J. Davenport, H.S. Isaacs, B.M. Ocko, *Science* 255 (1992) 1416.
- [30] T. Kondo, J. Morita, K. Hanaoka, S. Takakusagi, K. Tamura, M. Takahasi, J. Mizuki, K. Uosaki, *J. Phys. Chem. C* 111 (2007) 13197.
- [31] M. Takahasi, Y. Hayashi, J. Mizuki, K. Tamura, T. Kondo, H. Naohara, K. Uosaki, *Surf. Sci.* 461 (2000) 213.
- [32] K. Uosaki, S. Ye, T. Kondo, H. Naohara, in: M.P. Soriaga, J. Stickney, L.A. Bottomley, Y.-G. Kim (Eds.), *Thin Solid Films: Preparation, Characterization, Applications*, Kluwer Academic/Plenum Publishers, New York, 2002.
- [33] M. Takahasi, K. Tamura, J. Mizuki, T. Kondo, K. Uosaki, *J. Phys. Condensed Matter* (2010), in press.
- [34] T. Kondo, J. Morita, M. Okamura, T. Saito, K. Uosaki, *J. Electroanal. Chem.* 532 (2002) 201.
- [35] T. Kondo, S. Takakusagi, K. Uosaki, *Electrochem. Commun.* 11 (2009) 804.
- [36] T. Kondo, K. Tamura, M. Takahasi, J. Mizuki, K. Uosaki, *Electrochim. Acta* 47 (2002) 3075.
- [37] T. Kondo, K. Tamura, S. Takakusagi, K. Kitamura, M. Takahasi, J. Mizuki, K. Uosaki, *J. Solid State Electrochem.* 13 (2009) 1141.
- [38] D.J. Tweet, K. Akimoto, T. Tatsumi, I. Hirose, J. Mizuki, J. Matsui, *Phys. Rev. Lett.* 69 (1992) 2236.
- [39] Y.S. Chu, H. You, J.A. Tanzer, T.E. Lister, Z. Nagy, *Phys. Rev. Lett.* 83 (1999) 552.
- [40] M. Takahasi, J. Mizuki, *Phys. Rev. Lett.* 96 (2006) 055506.
- [41] A. Menzel, K.-C. Chang, V. Komanicky, H. You, Y.S. Chu, Y.V. Tolmachev, J.J. Rehr, *Rad. Phys. Chem.* 75 (2006) 1651.
- [42] S. Ye, C. Ishibashi, K. Uosaki, *Langmuir* 15 (1999) 807.